Transitions and Relaxations in Poly(2,6-diphenyl 1,4-phenylene ether)

Wolfgang Wrasidlo*

Materials Sciences Laboratory, Boeing Scientific Research Laboratories, Seattle, Washington 98124. *Received June 10, 1971*

ABSTRACT: The thermal behavior of poly(2,6-diphenyl 1,4-phenylene ether) was studied over a temperature range from −170 to 500° by means of dynamic calorimetric, volumetric, mechanical, and dielectric techniques. The polymer shows no transitions or relaxations below 100°, a solid-state transition at 118°, a glass transition at 220°, a premelt transition at 365°, and a melt transition at 481°. Cold crystallization in amorphous samples occurs above the glass-transition interval, resulting in semicrystalline polymers of various degrees of crystallinity and crystal perfection. Data on heat capacities, heat of crystallization, enthalpy and entropy of fusion, and coefficient of thermal expansion are presented. The results of various test methods are compared and possible origins of transitions and relaxations are identified.

The physical properties of polymers vary with temperature depending on the kind and degree of inter- and intramolecular interactions of polymer chains or chain segments. It is of interest to know what motions are responsible for property changes and how they relate to the chemical structure of polymers. Polymers composed entirely of aromatic units offer unique opportunities for studying molecular motion. Internal rotations of chain segments, believed to cause transitions and relaxations in ordinary polymers, are greatly restricted in fully aromatic polymers owing to resonance and substituent effects and the high moment of inertia of aromatic rings.

An interesting and important family of aromatic polymers is the polyphenylene ethers. Although a variety of these polymers have been synthesized,[1] only poly(2,6-dimethyl 1,4-phenylene ether) has become of commercial importance. Consequently, the physical properties of this polymer have been studied extensively and several papers have disclosed its thermodynamic,[2-6] dynamic-mechanical,[7,8] and dielectric properties.[9] A structural homolog of this polymer, poly(2,6-diphenyl 1,4-phenylene ether) is the subject of this paper. Initially, we intended simply to screen the properties of this polymer in conjunction with some studies on other aromatic polymers. However, the initial results, particularly the differential thermal analysis data, appeared intriguing enough to encourage us to examine this polymer in detail.

Experimental Section

Material and Sample Preparation. The polymer was produced by the General Electric Co. and has the structure I. The intrinsic viscosity determined in chloroform at 25° was 1.05, from which a

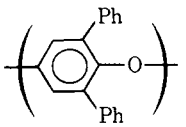

I

viscosity-average molecular weight of 143,000 was calculated. The "as received" clear film specimens were lightly tan colored, indicating the presence of trace amounts of impurities (*i.e.*, possibly copper salt catalysts and quinone oxidation products). The polymer was purified by the following procedure. Charcoal (0.5 g) was added to a turbid orange solution of crude polymer (20 g) in *sym*-tetrachloroethane (300 ml) and the mixture was stirred under reflux for 2 hr. The solution was filtered with suction through a coarse sintered-glass Büchner funnel containing a 5-mm thick layer of celite. The clear, colorless filtrate was cooled to room temperature and the polymer was quenched by adding 300 ml of ethyl alcohol to yield a white flocculent precipitate which was dried at 100° under reduced pressure. Film specimens were prepared by casting 15% *sym*-tetrachloroethane solutions of purified polymer onto glass plates and drying at 50° for 4 hr, followed by heating at 150° under reduced pressure for 3 hr.

Crystallization. Cold crystallization was achieved by heating films between two plate furnaces in an inert atmosphere to specified temperatures and heating isothermally for various periods of time. Specimens were annealed at controlled, linear cooling rates as indicated in Table I. The furnace temperature was controlled by a silicon-controlled rectifier circuit and the temperature was recorded *via* a thermocouple located at the surface of the sample. The time periods for crystallization at temperatures in excess of 420° were reduced to prevent decomposition. Attempted melt crystallization under isothermal conditions (sample 8) resulted in some decomposition, and consequently no crystallization was achieved.

Measurements. Differential thermal analysis was performed on a Du Pont unit (Model 900) using the scanning calorimeter. Film samples 0.015 cm thick were cut into circular disks, placed into the sample holder capsule, and hermetically sealed. Runs were made at a heating rate of 10°/min using 30-mg samples. In this way the heat of melting gave peak heights >2 in. on the 0.5°/in. ΔT scale. The melting point was determined by extrapolating the linear portion of the melting peak back to the base line.

The glass-transition temperature was determined at various heating rates from the inflection point of the endothermic discontinuity in base line (ΔT sensitivity, 0.2° /in.). Since the location of this point along the temperature axis depended upon heating rates, the corrected T_g^0 was obtained by extrapolating the data to zero heating rate.

The heats of crystallization and melting were measured using the time-base accessory of the instrument and applying the procedure described in the instrument manual. Calibration coefficients were determined for tin, indium, lead, and zinc. The heats of fusion

* Address correspondence to Gulf Energy and Enviromental Systems, San Diego, Calif. 92112.

(1) A. S. Hay, P. Sherian, A. C. Cowan, P. F. Erhardt, W. R. Haaf, and J. E. Theberge, "Encyclopedia of Polymer Science," Vol. 10, Interscience, New York, N. Y., 1969, p 92.
(2) F. E. Karasz and J. M. O'Reilly, *J. Polymer. Sci., Part B*, **3**, 561 (1965).
(3) F. E. Karasz, H. E. Bair, and J. M. O'Reilly, *ibid., Part A*, **6**, 1141 (1968).
(4) F. E. Karasz and D. Mangaraj, *Polym. Prepr., Amer. Chem. Soc., Div. Polym. Chem.*, **12**, 317 (1971).
(5) A. R. Shultz and C. R. McCullough, *J. Polym. Sci., Part A-2*, 7, 1577 (1969).
(6) A. R. Shultz, *ibid., Part A-2*, **8**, 883 (1970).
(7) J. K. Gillham and R. E. Schuseuker, *Appl. Polym. Symp.*, **2**, 59 (1966).
(8) R. Mattes and E. Rochow, *J. Polym. Sci., Part A*, **3**, 375 (1966).
(9) C. R. Reed, *Polym. Prepr., Amer. Chem. Soc., Div. Polym. Chem.*, **12**, 218 (1971).

TABLE I
COLD CRYSTALLIZATION OF
POLY(2,6-DIPHENYL 1,4-PHENYLENE ETHER)

Sample no.	Heating rate, °C/min	Cooling rate, °C/min	Crystallization temp, T_c	Time at T_c	X-Ray crystallinity, %
1	20	0.5	230	2 hr	0
2	20	0.5	250	2 hr	15
3	20	0.5	275	2 hr	23
4	20	0.5	320	2 hr	33
5	20	5.0	320	2 hr	22
6	20	0.5	420	30 min	44
7	20	0.5	452	30 min	52
8	40	5.0	480	30 min	
9	40	0.75	480	10 min	0

calculated for these metals agreed within ±3% of the literature values.[10] Sample size and ΔT sensitivities were such that the curve areas were at least 3 in.^{2}.

Specific heats were measured on the same instrument according to a procedure described by Wunderlich.[11] Heat capacity calibration curves were obtained on sapphire disks using the values of Ginnings and Furakawa on specific heats of aluminum oxide.[12] The temperature axis of the recorder was calibrated using A. H. Thomas organic calibration standards. The melting points obtained agreed within ±0.5° of the recorder readout. The asymmetry of the sample cell was determined using empty aluminum capsules of equal weights. Deflections of about 0.05 in. at the highest instrument sensitivity (0.004 mV/in.) were recorded. Polymer samples were run at a heating rate of 10°/min in a helium atmosphere at a flow rate of 0.1 l./min. The standard deviation of averages of three runs from a smooth curve was ±3% and the internal precision of the instrument was ±2%.

Dynamic-mechanical data were obtained on a longitudinal apparatus (Vibron DDV II) at various fixed frequencies. The commercial instrument was modified for high-temperature operation. The instrument produces a sinusoidal tensile strain on one end of the specimen from which the phase angle, δ, of the strain against the stress generated on the other end of the specimen was measured. The dynamic loss (E'') and storage (E') moduli were then calculated from the strain and stress amplitudes.

Dielectric measurements were made on an apparatus developed in our laboratory. A detailed description of the device is presented elsewhere.[13] A dielectric test cell was constructed with internal heaters for operation up to 500° at linear heating rates ranging from 0.5 to 40°/min. The cell consisted of a two-terminal electrode system with shielded small-diameter wire leads connected to the measuring circuit. Specimens consisting of circular disks 0.006 in. thick and 1.8 in. in diameter sandwiched between aluminum foil 0.0002 in. thick were placed into the electrode assembly under light spring pressure (~1.2 lb). Recordings of dissipation factor (tan δ) and capacitance were made as a function of temperature.

X-Ray data were generated on a Siemens counter diffractometer. Diffraction patterns (reflection geometry) of specimens 0.015 cm thick, varying in amorphous and crystalline content (Table I) were recorded over an angular range (2θ) from 6 to 45°. This range encompasses the intensities of both the crystalline reflections (I_c) and the principal amorphous halo (I_a). To resolve the crystalline and amorphous scattering, a method developed by Challa, Hermans, and Weidinger was employed,[14] and the fractional crystallinities were obtained from regression curves based on I_c and I_a. Flat-plane X-ray photographs (Cu $K\alpha$ radiation) were obtained after exposure times of 4 hr at a specimen-to-film distance of 5 cm. (Details of the X-ray data will be published in a separate paper in the near future.)

Freezing point depression experiments of 2, 4, and 6 wt % solutions of polymer (sample 7 of Table I) in 1-chloronaphthalene were performed using a conventional setup.

Thermal expansion measurements were made on a Du Pont thermomechanical analyzer (Model 940). The instrument was modified to extend the temperature range to 600°. Samples were prepared by extruding bulk material at 230° under 12,000-psi pressure through a 4-mm orifice followed by quenching the rods in a 2-propanol–Dry Ice mixture. Cylindrical specimens were then cut on a lathe and the surfaces polished with emery cloth.

Electron micrograph and diffraction patterns were obtained on a Philips instrument at 100 kV at a magnification of 38,000×. Specimens were prepared by placing a drop of a 2% solution of amorphous polymer in chloroform onto the copper grids and evaporating the solvent at ambient temperature. 100% amorphous film samples (~10^{-4}–10^{-5} in. thick) were obtained which were cold crystallized by heating in a nitrogen atmosphere to 450° at a heating rate of 5°/min followed by annealing at 450° for 30 min and cooling at a programmed linear heating rate of 0.2°/min.

Results

Prior to property measurements the thermal stability was tested by simultaneous differential thermal and thermogravimetric analysis on a Mettler universal thermal analyzer. Figure 1 is a recorder trace of a thermogram obtained on a 10-mg powdered sample between 25 and 1000° at a heating rate of 10°/min. The onset of decomposition is marked at 515° by a strong endothermic reaction resulting in simultaneous weight loss. Decomposition reaches a maximum rate of 6.2%/min at 550° (DT 6). Based on these data, the possibility of degradation during dynamic measurements up to 500° at comparable heating rates was excluded. However, since decomposition of this polymer was only 25° above its melting point, the experimental time scales of all subsequent high-temperature measurements were kept as short as possible and samples were protected from air oxidation by conducting experiments in inert atmospheres.

In Figure 2 are four recorder traces of differential temperature *vs.* temperature of 32-mg samples with varying degrees of crystallinity and crystal perfection. A scan of 100% amorphous polymer ($0X_c$) shows clearly the appearance of the glass-transition interval between 220 and 230°, resulting in an endothermic discontinuity in the base line, an exothermic region between 258 and 290° with a peak at 278° due to the

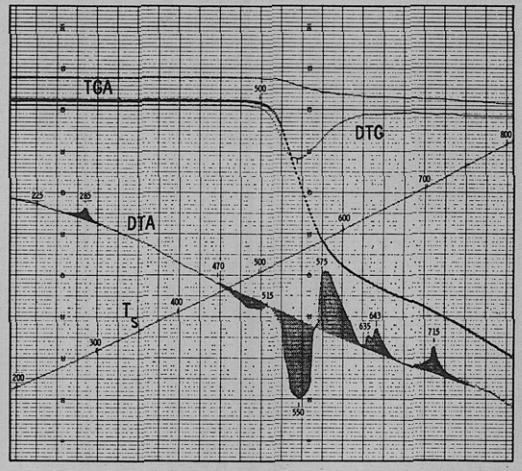

Figure 1. Recorder trace of simultaneous tga/dta of a 32.3-mg sample at a heating rate of 10°/min in a helium atmosphere.

(10) "American Institute of Physics Handbook," 2nd ed, McGraw-Hill, New York, N. Y., 1963, pp 4–66.
(11) B. Wunderlich in "Differential Thermal Analysis," Part IV, A. Weissberger, Ed., in press, Chapter 17.
(12) D. C. Ginnings and G. T. Furakawa, *J. Amer. Chem. Soc.*, **75**, 522 (1953).
(13) W. Wrasidlo, *J. Polym. Sci., Part A-2*, in press; Boeing Scientific Research Laboratories Report No. D1-821038, 1971.
(14) G. Challa, P. H. Hermans, and A. Weidinger, *Makromol. Chem.*, **56**, 1654 (1959).

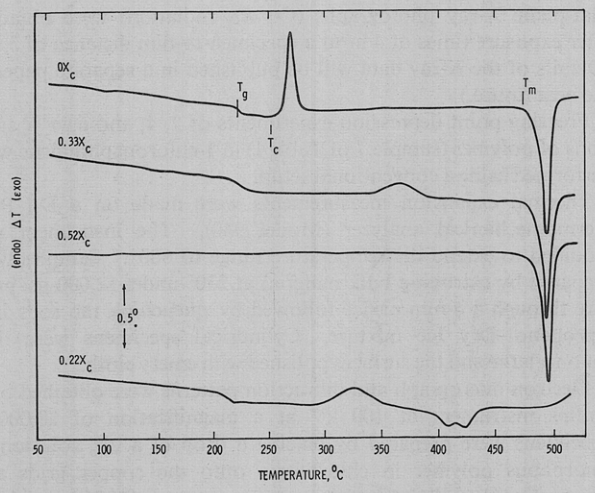

Figure 2. Recorder trace of differential thermal analysis of samples with varying degrees of crystallinity and crystal perfection.

heat of crystallization, and an endothermic region between 480 and 510° with a peak at 497° attributed to melting. Curve no. $0.33X_c$ was obtained from a sample whose thermal history is described in Table I (sample no. 4). The glass-transition temperature of this sample appears at approxi-

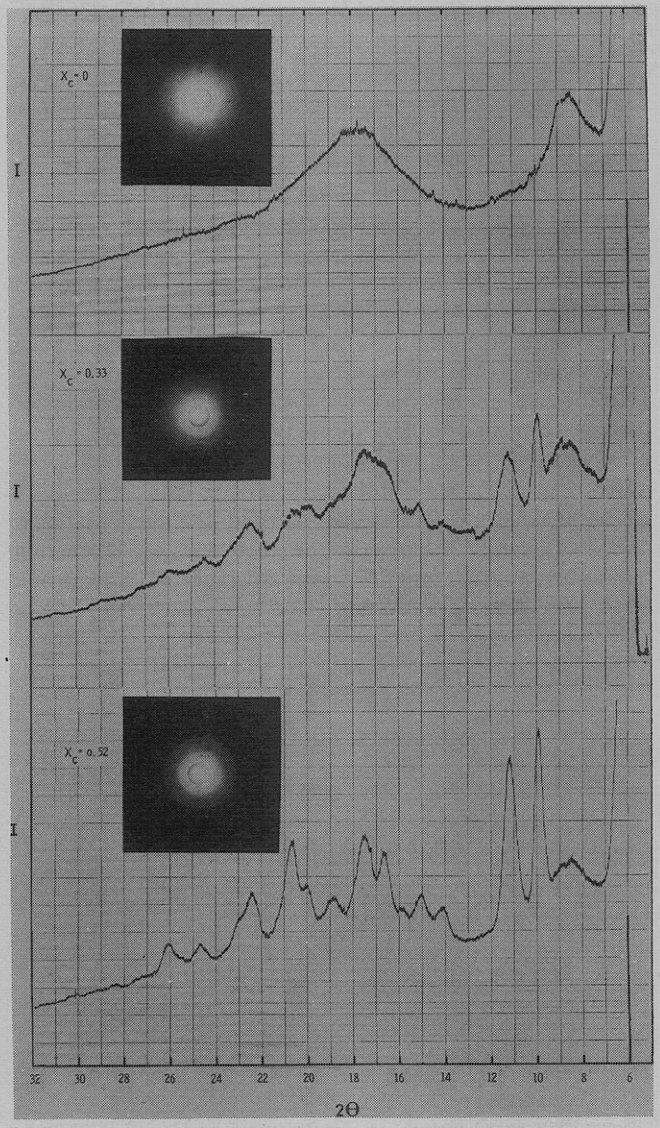

Figure 3. X-Ray diffraction pattern of samples with varying crystallinities.

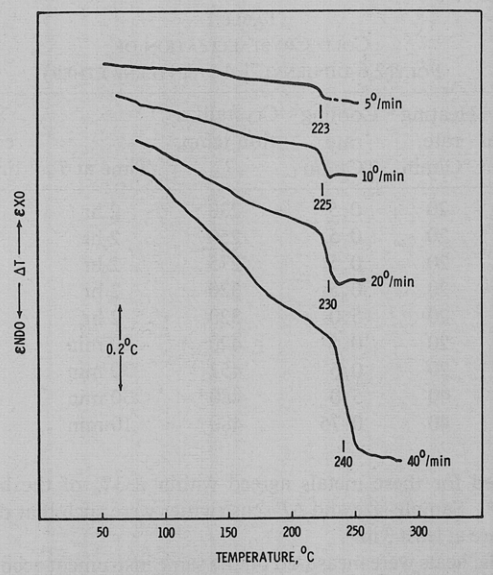

Figure 4. Recorder trace of differential thermal analysis at various heating rates.

mately the same ΔT intensity and in the same temperature range as for the amorphous polymer. An exothermic region with a peak at 320° is due to additional crystallization during measurement; the location and peak area of the melting endotherm are very similar to those of the "originall" amorphous polymer (curve $0X_c$). The data of polymer sample no. 7 (Table I) with X-ray crystallinity of 52% is shown in the third curve. The only transition observed in this sample is melting. X-Ray diffraction patterns for these samples are shown for comparison in Figure 3. The fourth curve ($0.22X_c$) in Figure 2 was obtained from sample no. 5 (Table I). The thermal history of this sample is similar to that of sample no. 4 except that the cooling rate was ten times faster. Some striking difference in the thermal behavior of this sample compared to sample no. 4 was noted. The crystallization exotherm occurred at 308°, 40° lower than that for sample no. 4. The melting peak at 495° disappeared completely and, instead, a melting region appeared in the form of an endothermic doublet with peaks at 421 and 435°, respectively. There are several reasons for the lowering of the melting temperature and multiple peaks. Higher cooling rates could produce crystals in the polymer with two degrees of perfection, while the lowering in the melt temperature suggests the presence of a rather metastable crystalline phase.

The glass-transition interval of completely amorphous polymer was examined in more detail. The effect of heating rate on the intensity and location of the endotherm is shown in Figure 4. As expected, for every doubling in heating rate a

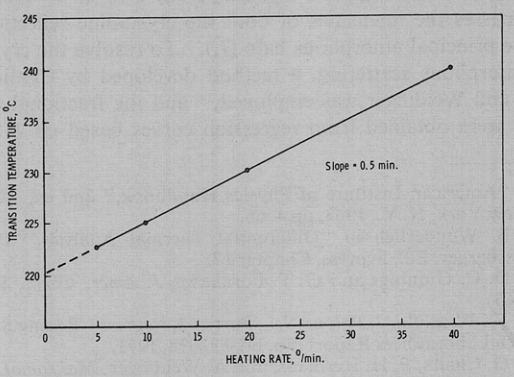

Figure 5. Plot of glass-transition temperature *vs.* heating rate.

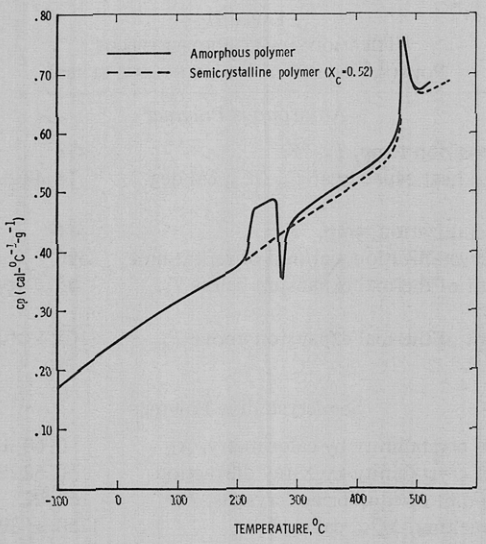

Figure 6. Heat capacity of amorphous and semicrystalline sample ($X_c = 0.52$).

twofold increase in ΔT and a shift of these curves toward higher temperatures were observed. The plot in Figure 5 shows a linear relationship of T_g with heating rate. An arbitrary extrapolation of the line to the ordinate axis gave a value of 220° for the "corrected" glass-transition temperature.

A more quantitative description of the glass-transition interval is given in Figure 6, where the heat capacity (C_p) is plotted as a function of temperature. Below the T_g, the heat capacity is a smooth function of temperature and is similar for both the amorphous and crystalline polymers. However, in the T_g interval of about 20° in width, a jump in C_p of 0.067 cal/(°C g) was observed in the amorphous polymer, from which a value of 4.11 cal/mol of bead was calculated. A hypothetical bead was defined as the smallest molecular segment connected to the chain by flexible bonds.

The dynamic-mechanical properties were measured at fixed frequencies of 3.5, 11, 35 and 110 cps. Figure 7 shows the dynamic tensile (E') and loss (E'') moduli of semicrystalline ($X_c = 0.52$) polymer plotted as a function of temperature. Between −170° and ambient temperature, E' decreases smoothly from 4.5×10^{11} to 3.2×10^{11} dyn/cm². This small decrease in E' is attributed to thermal expansion of the specimen. The spectrum of completely amorphous material between 25 and 400° shows a weak and broad relaxation from 100 and 150° with a loss maximum at 130° and a pronounced loss region between 190 and 285° with a maximum in E'' between 230 and 240°, depending upon the applied frequency. The temperature dependence of the loss maximum on frequency was only 10° within the experimentally attainable frequency range, certainly not enough to permit the calculation of an activation energy for this relaxation process to any reasonable accuracy. Nevertheless, since the mechanical loss occurs in the glass-transition interval of this polymer, it is undoubtedly due to a relaxation mechanism involving long-range cooperative chain motion in the amorphous phase. The influence of crystalline regions in depressing this relaxation was also demonstrated with sample no. 7. An increase in crystallinity to 52% not only reduces the magnitude of the mechanical loss, but also produces a significant shift toward higher temperatures.

Figure 8 is a recorder trace of the dielectric dissipation factor (tan δ_E) and capacitance of a 0.006-in. film specimen of amorphous polymer plotted *vs.* temperature. The relaxa-

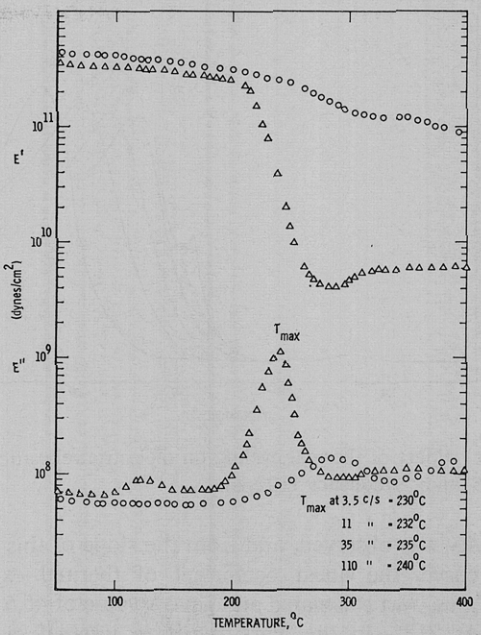

Figure 7. Dynamic-mechanical relaxation spectrum of amorphous and semicrystalline film specimen at a heating rate of 5°/min and a frequency of 110 cps (other frequency data listed).

tion spectrum exhibits three pronounced loss maxima at 288, 338, and 485°, and a weak but still detectable relaxation maximum at 125°. The peak at 288° disappears completely on heating to 300° and is attributed to a relaxation involving crystallization (note: not crystallinity), and the 485° maximum is due to a melt relaxation. However, the weak band at 125° and the strong absorption at 338° are presently not well understood. Thermal cycling a sample to temperatures as indicated in Figure 9 results in successive shifts of the 338° band to higher temperatures with only a slight increase in magnitude. While the increase in temperature is undoubtedly due to increasing crystallinity, the almost constant amplitude suggests that dipoles in both the amorphous and crystalline phases contribute to this relaxation.

The results of thermal expansion measurements of an amorphous sample over a temperature range from −170 to 500° are shown in Figure 10. Between −170 and 100° the expansivity is an almost linear function of temperature with no apparent transition. At 118°, a small but distinct change in probe displacement occurred, indicating a solid-state transition. Between 118 and 220° a fairly linear response in

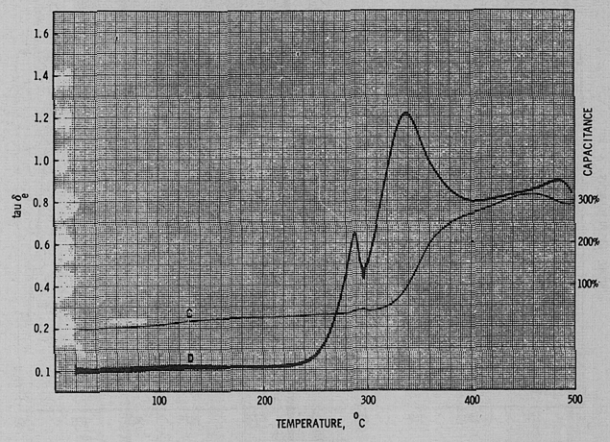

Figure 8. Recorder trace of dielectric loss tangent and capacitance *vs.* temperature at a heating rate of 5°/min and a frequency of 190 cps.

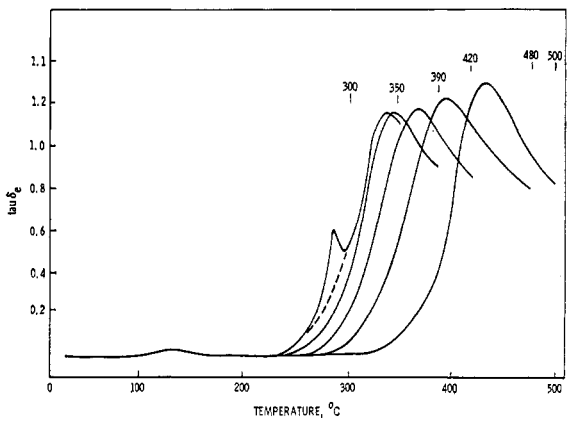

Figure 9. Effect of thermal cycling on dielectric relaxation (heating rate 5 °/min; frequency 110 cps).

expansivity was observed, and from the slope of this portion of the curve, the linear coefficient of thermal expansion below T_g, α_0, was calculated and gave a value of 45.5×10^{-6} °C^{-1}. At 215°, in the glass-transition interval, a drastic increase in α occurs, resulting in a sigmoid-shaped curve. Then between 245 and 350° the expansivity changes again quite linearly with temperature, permitting the calculation of the linear coefficient of thermal expansion above the T_g ($\alpha_1 = 102 \times 10^{-6}$ °C^{-1}). Above 350° a third, but more gradual, change in the thermal expansion occurs until the melting range is approached and the curve exhibits a steep negative slope due to loss in the shape of the sample.

Discussion

A summary of thermodynamic properties of poly(2,6-diphenyl 1,4-phenylene ether) is given in Table II. Particular care was taken in purifying the polymer by removing trace metal salt catalysts and possible quinone oxidation products whose presence is known[9] to interfere with dielectric measurements and could result in mechanical relaxations. Measurements were made by means of dynamic methods, and therefore the nonequibilibrium aspects of transitions and relaxations will be emphasized. The reader should be aware that the nonequilibrium techniques employed in this study made it possible to determine the high-temperature thermodynamic properties such as heat capacities, melting points, heats of melting and fusion, the entropy of fusion, and associated mechanical and dielectric relaxations. With this polymer, all these properties simply cannot be determined by conventional equilibrium methods such as adiabatic calorimetry or isothermal relaxation techniques. Furthermore, it was precisely through the use of dynamic thermal analysis that the stability of the physical structure of this polymer was fully realized and demonstrated (see Figures 1, 4, and 11).

TABLE II
THERMODYNAMIC PROPERTIES OF POLY(2,6-DIPHENYL 1,4-PHENYLENE ETHER)

Amorphous Polymer	
Glass-transition temp, T_g, °K	493
Change in heat capacity at T_g, ΔC_p, cal deg^{-1} mol^{-1}	16.48 ± 0.5
Cold crystallization temp, °K	>500
Heat of crystallization, cal/mol of repeat unit	596
Coefficient of thermal expansion below T_g, α_0, °C^{-1}	45.5×10^{-6}
Coefficient of thermal expansion above T_g, α_1, °C^{-1}	102×10^{-6}
Semicrystalline Polymer	
Degree of crystallinity by calorimetry, X_L	0.60 ± 0.05
Degree of crystallinity by X-ray diffraction	0.52 ± 0.10[a]
Melting point of equilibrium crystals, T_m^0	757 °K
Heat of melting, ΔQ_m, cal mol^{-1}	1750 ± 30
Heat of fusion, $\Delta Q_m/X_c$, cal mol^{-1}	2916 ± 120
Entropy of fusion, $\Sigma\Delta S_{f,tr}$, cal deg^{-1} mol^{-1}	3.85 ± 0.2
T_g^0/T_m^0	0.69

[a] This value corresponds to cold crystallizability.

A comparison of the heat capacity of quenched amorphous with semicrystalline polymer is presented in Figure 6. Both polymers had identical heat capacities up to 220°, the glass-transition temperature, indicating that crystallinity and chain conformation did not contribute to C_p. The glass-transition interval in the amorphous sample shows a discontinuous jump in heat capacity (ΔC_p) of 16.48 ± 0.5 cal deg^{-1} mol^{-1}, cor-

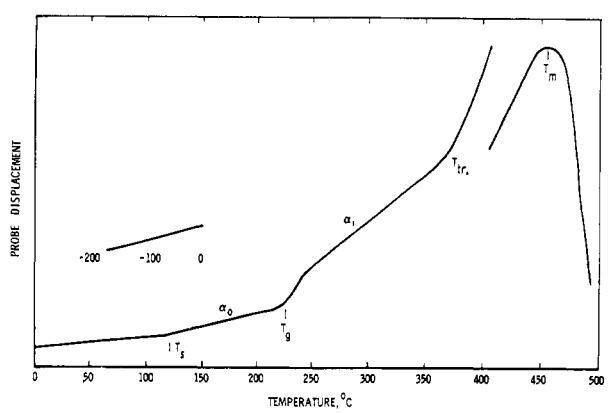

Figure 10. Recorder trace of thermal expansion *vs.* temperature (heating rate 5 °/min, He atmosphere).

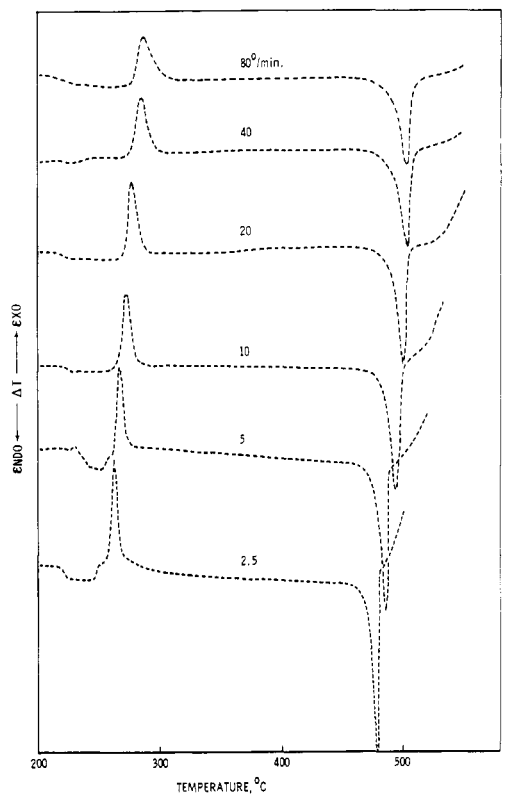

Figure 11. Effect of heating rate on cold crystallization, melt transition, and thermal decomposition temperatures.

responding to approximately four hypothetical beads, in agreement with the repeat unit structure of this polymer (*i.e.*, assuming that Wunderlich's rule of constant C_p[15] holds for this type of polymer). Above the crystalline region from 300° and up to the melting range, the original amorphous and the isothermally cold-crystallized semicrystalline polymer behave quite similarly, the heat capacity of the isothermally crystallized sample being only 2% lower than that of the amorphous sample.

An effort was made to test the metastability of the crystalline phase by dta at drastically different heating rates. In order to avoid errors due to data reduction, the magnitude of the crystallization exotherms and melt endotherms (Figure 11) was adjusted by changing the sample weight and instrument sensitivity in such a way as to keep the anticipated peak areas constant. In this way it was possible to determine the onset of crystallization and melting as outlined in the Experimental Section.

Substantial increases in crystallization temperatures from 235 to 280° were observed on increasing the heating rates from 2.5 to 80°/min. On the other hand, the difference in onset of melting between the slowest and fastest heating rate was only 7°. When considering the fact that crystallization conditions were drastically different, thus leading very likely to a larger distribution of crystal sizes at the higher heating rates, the melting points remained surprisingly constant. As stated by Wunderlich and Baur,[15] several interpretations are possible including (a) the formation of equilibrium crystals which show no superheating, (b) the formation of metastable crystals with no rearrangement or recrystallization, or (c) the range of heating rates employed being too small, resulting in compensation of superheating and reorganization. In view of the wide range of heating rates employed in our work, we conclude that reorganization of the metastable crystals is extremely slow in our case.

The low entropy of fusion (Table II) led to the interpretation that the molten state is of long-range order similar to that of the semicrystalline solid state and only minor conformational changes take place during melt transitions. When examining these conclusions in the light of the very large differences in observed X-ray crystallinities, it becomes quite apparent that the present operational definitions of order are inadequate.

Thermal expansion data of a quenched, amorphous, bulk sample are shown in Figure 10. In the temperature range from −170 to 100°, the data agree with heat capacity measurements, since no transitions were observed. The glass transition is clearly apparent from the expansion curve, showing a discontinuity in α. Above T_g the coefficient of linear thermal expansion α_l has a magnitude characteristic of liquids, of the order of 10^{-3} deg^{-1}; below T_g α is smaller by a factor of 2. The melt transition is also obvious from Figure 10, resulting in a steep drop in probe displacement due to the loss of shape of the sample. However, there are two additional transitions observed in the expansion curve which are not apparent from C_p measurements. First, a weak but sharp discontinuity at 118° suggests a solid-state transition and also results in weakly active dielectric and dynamic-mechanical relaxations (Figures 7 and 8). Mechanical relaxations in this temperature range have previously been reported[16] for poly(2,6-dimethyl 1,4-phenylene ether) at acoustic frequencies. These workers observed a weak damping maximum at 100° and from the temperature dependence of frequency calculated an activation energy of 20 kcal/mol for this relaxation process.

Based on these results, these investigators attribute this process to phenyl group oscillation. On the assumption that such torsional oscillation of phenyl groups results in different local conformations, passing from one to another over energy barriers, one can envision frequency-dependent viscoelastic behavior as a result of such transitions. However, we question the general significance of this relaxation, as other polymers containing chain phenylene moieties do not exhibit mechanical losses below the glass-transition temperature.[13] The feasibility of other than internal motions such as decoupling of local entanglements, motions specific to chain folds, or impurity effects such as end groups or oligomeric species should be considered.

A more gradual but strong change in the slope of the expansion curve occurs between 350 and 375°. This region constitutes a real transition rather than a mere deviation of the expansivity from linearity (*i.e.*, a distinct penetration displacement at 365° was also observed when a run was made by using the penetration rather than expansion probe). The nature of this submelt transition is presently not well understood. However, since a strong dielectric relaxation is also observed at this temperature (Figure 8) and since the magnitude of this relaxation mode remains constant with increasing crystallinity (Figure 9), it is plausible that this volume expansion originates in dipole motion of both the amorphous and crystalline phases. A possible explanation is that the motions involved are relative translations resulting in association–disssociation of chains or chain segments in the direction parallel to the chain axis. Such motions are guaranteed by symmetry (end effects neglected) to result in equivalent equilibrium energy states separated by a barrier,[17] and therefore should contribute only a constant amount to the heat capacity.

An alternate and probably more realistic explanation for this premelt transition is the onset of a rotorphase which would give rise to a change in crystal structure from monoclinic (Figure 12) to hexagonal close packing. This motion would result in a lattice expansion consistent with the observed results. The appearance of strongly active dielectric relaxations in this temperature range can also be explained by a mechanism involving dipole rotations. The absence of a

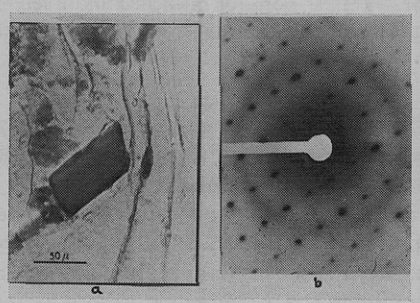

Figure 12. Single crystal of poly(2,6-diphenyl 1,4-phenylene ether). (a) Electron micrograph of a thin-film sample of poly(2,6-diphenyl 1,4-phenylene ether), cold crystallized at 450°. Central portion shows single crystal (magnification = 66,000×). (b) Electron diffraction pattern from a single crystal showing about 50 lattice deflections. The crystal structure deduced from this pattern is monoclinic.

(15) B. Wunderlich and A. Baur, *Advan. Polym. Sci.*, 7, 281 (1970).
(16) S. DePetris, V. Frosini, E. Butta, and M. Baccaredda, *Makromol. Chem.*, **109**, 54 (1967).
(17) R. L. McCullough and J. J. Hermans, *J. Chem. Phys.*, **45**, 1441 (1966).

TABLE III
TRANSITION TEMPERATURES[f] OF POLY(2,6-DIPHENYL 1,4-PHENYLENE ETHER) BY VARIOUS METHODS

Method	Measurement	T_s,[c] °C	T_g, °C	T_c,[d] °C	T_{tr},[e] °C	T_m, °C
Dsc	C_p	N.o.[a]	225	258	N.o.	481
Tma	α	118	225	N.o.	350–375 (not distinct)	470
Dma	E'' [b]	130	230	285	N.o.	Not attainable by this method
Dsde	ϵ'' [b]	125	N.o.	288	338	485

[a] N.o. = not observed. [b] Applied frequency = 110 cps. [c] Onset of a solid-state transition. [d] Temperature of maximum in crystallization exotherm. [e] Onset of premelt transition. [f] Reported values were all from measurements at a heating rate of 5 °C/min.

jump in the heat capacity for such a transition is more difficult to accept. However, since this transition is more gradual (*i.e.*, the dielectric loss peak extends over a 150° range) it is probably not detectable by heat capacity measurements.[18]

A summary of transition and relaxation temperatures is given in Table III. It was shown that a complete description of transitions and relaxations necessitates the use of samples of well-defined thermal histories and the application of various experimental techniques at comparable experimental conditions. The importance of heat capacity measurements in assigning the glass-transition temperature of this polymer was clearly demonstrated. In the absence of C_p data it would have been difficult to guess which of the four discontinuities in the thermal expansion curve corresponds to the T_g.

On the other hand, thermal expansion data lead to the assignment of a subglass and submelt transition which could not be detected by differential scanning calorimetry. Dynamic-mechanical and dielectric relaxation spectra were useful in identifying possible origins of motion in transition regions of this polymer and in demonstrating the effects of changing morphology on these time-dependent processes.

(18) B. Wunderlich, *Kolloid-Z. Z. Polym.*, **231**, 605 (1969).

Thermal Transitions in Stereoisomers of Poly(*tert*-butyl ethylene oxide)

Namassivaya Doddi, W. C. Forsman,* and C. C. Price

Department of Chemistry, School of Chemical Engineering and Laboratory Research on the Structure of Matter, University of Pennsylvania, Philadelphia, Pennsylvania, 19104.
Received January 8, 1971

ABSTRACT: Differential scanning calorimetry was used to study thermal transitions in isotactic and base-catalyzed poly(*tert*-butyl ethylene oxide). The isotactic polymer had an equilibrium melting point of 135 ± 1° and a glass transition of 58 ± 1° which was verified with vibrating-reed measurements. It could be quench cooled from the melt, however, to give an amorphous polymer with a glass transition of 40 ± 1°. Upon aging, the thermograms of the quenched polymer developed an (anomalous) endothermic T_g which was explained in terms of the rate processes involved in passing through the glass transition. Base-catalyzed polymer demonstrated an equilibrium melting point of 63 ± 1° and a normal-appearing glass transition of −9 ± 1° both for quenched and freeze-dried samples. Heat capacities were calculated and tabulated over the temperature range of 0–180°, and are shown graphically in the regions of the thermal transitions.

Preparations of two stereoisomers of poly(*tert*-butyl ethylene oxide) having distinctly different physical properties have been reported in the literature.[1-5] Price and Fukatani[1] interpreted from nmr and X-ray data that the crystalline polymer prepared by coordination catalyst (Et_2Zn–H_2O) is isotactic, and the crystalline polymer prepared by base catalyst (*tert*-BuOK) is syndiotactic. Further investigation in this laboratory[6] and by Tani and Oguni[7] showed, however, that there must be approximately equal percentages of isotactic and syndiotactic dyads in the base-catalyzed polymer. Since it is semicrystalline, it must be made up of stereoblocks of isotactic and syndiotactic placements.

Since the reported value[8] for the glass transition of the isotactic polymer (35°) was considerably different than the values determined in this laboratory (53°), we decided a careful study of the thermal transitions in both stereoisomers was called for. We thus determined the glass transition of an annealed semicrystalline isotactic poly(*tert*-BuEO) specimen using the vibrating-reed technique.[9] We also measured specific heats, heats of fusion, and glass transitions of annealed and quenched isotactic and base-catalyzed semicrystalline

(1) C. C. Price and H. Fukutani, *J. Polym. Sci., Part A-1*, **6**, 2653 (1968).
(2) J. M. Bruce and S. J. Hurst, *Polymer*, **7**, 1 (1966).
(3) G. Allen, *et al.*, *ibid.*, **8**, 385 (1967).
(4) C. C. Price and D. Carmelite, *J. Amer. Chem. Soc.*, **88**, 4039 (1966).
(5) E. J. Vandenberg, U. S. Patent 3,285,861 (Nov 15, 1966).
(6) B. Furie, Ph.D. Thesis, Department of Chemistry, University of Pennsylvania.
(7) H. Tani and N. Oguni, *J. Polym. Sci., Part B*, **7**, 803 (1969).
(8) G. Allen, *et al.*, *Polymer*, **8**, 406 (1967).
(9) P. E. Wapner and W. C. Forsman, *Trans. Soc. Rheol.*, in press.